

Supplemental Material: Non-adiabatic Strong Field Ionization of Atomic Hydrogen

D. Trabert¹, N. Anders¹, S. Brennecke^{2,*}, M. S. Schöffler¹, T. Jahnke¹, L.

Ph. H. Schmidt¹, M. Kunitski¹, M. Lein², R. Dörner¹, and S. Eckart^{1†}

¹ *Institut für Kernphysik, Goethe-Universität, Max-von-Laue-Str. 1, 60438 Frankfurt am Main, Germany*

² *Institut für Theoretische Physik, Leibniz Universität Hannover, Appelstr. 2, 30167 Hannover, Germany*

(Dated: November 3, 2021)

I. ANALYTICAL EXPRESSION FOR THE INITIAL POSITION INCLUDING NON-ADIABATIC CORRECTIONS

The initial position \vec{r}_{SFA} can be determined from strong-field approximation (SFA) [1, 2]. For our non-adiabatic classical two-step (NACTS) simulations, we use the exact values for \vec{r}_{SFA} as starting points for the classical trajectories.

The initial position can also be approximated as (see Eq. (15) from Ref. [3]):

$$\vec{r}_{\text{SFA}}(\vec{p}_{\perp}, \vec{E}(t), \dot{\vec{E}}(t)) \approx -\frac{\vec{E}(t)}{2} \frac{p_{\perp}^2 + 2I_p}{|\vec{E}(t)|^2 - \vec{p}_{\perp} \cdot \dot{\vec{E}}(t)} \quad (\text{S1})$$

It is evident from Eq. (S1) that \vec{r}_{SFA} depends on the electron's initial momentum at the tunnel exit as well as the temporal evolution of the laser electric field and that \vec{r}_{SFA} and \vec{p}_{\perp} are correlated. This is illustrated in Fig. 3(b).

II. ADDITIONAL ELECTRON MOMENTUM DISTRIBUTIONS FROM MODIFIED SEMI-CLASSICAL MODELS

Fig. S1(a) shows the result from a classical two-step (CTS) simulation that is obtained as for Fig. 2(c) but here Coulomb interaction after tunneling is neglected. This leads to an angular distribution that is independent of p_r and that peaks at -90° and $+90^\circ$. These directions coincide with the negative vector potentials that correspond to the peaks of the magnitude of the laser electric field. Accordingly, for the data shown in Fig. S1(a) the offset angle α_{off} is zero for all p_r .

In Fig. S1(b) we show the result from our NACTS simulation as in Fig. 2(d) but here we use the initial position from the TIPIS model (see main text) instead of the initial position from SFA. It is evident from Fig. S1(b) that the non-adiabatic corrections of the initial position give rise to significant modifications of the electron momentum distribution. In particular, a fork-like structure is clearly visible in this distribution for radial electron momenta with $p_r > 0.85$ a.u. The fork-like structure is due to the mapping of the elliptically shaped electron momentum distribution to a cylindrical coordinate system and subsequent normalization. The branch of the

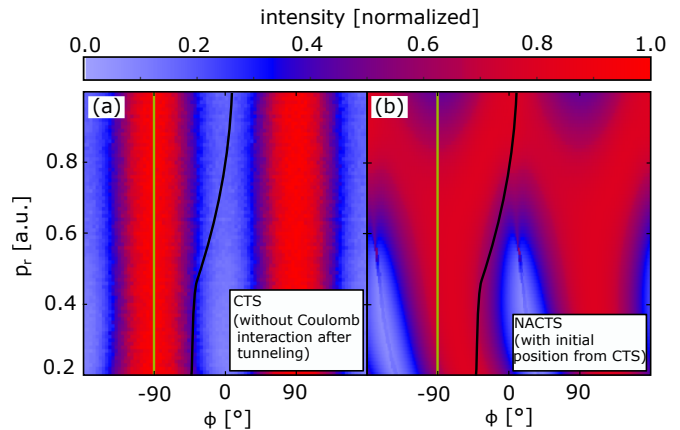


FIG. S1. (a) shows the row-wise normalized electron momentum distribution that is obtained from the CTS model modified by neglecting Coulomb interaction after tunneling. (b) shows the electron momentum distribution from our NACTS model modified by taking the initial position from the TIPIS model. The data is presented in full analogy to Fig. 2.

fork-like structure that belongs to higher angular offsets α_{off} shows a higher intensity leading to an overall shift towards higher angular offsets α_{off} and improving the agreement with the experiment and the TDSE simulation. In the full NACTS model (see Fig. 2(d)), the branch that belongs to higher angular offsets α_{off} shows an even higher intensity. This leads to higher angular offsets and shows the correct trend for α_{off} as a function of p_r that is in agreement with experiment and TDSE (see Fig. 2(a), 2(b) and 3(a)).

III. THE ANGULAR OFFSET α_{off} FOR DIFFERENT KELDYSH PARAMETERS γ

In Fig. S2 we show additional calculations for longer wavelengths and, hence, smaller Keldysh parameters compared to the parameters used in the main text. In the TDSE calculations, the angular offset α_{off} increases as a function of the radial momentum p_r for all studied laser parameters. This can be qualitatively reproduced using the NACTS model. For sufficiently adiabatic conditions (here for a Keldysh parameter of $\gamma = 0.5$) the CTS model with initial positions from TIPIS shows the correct trend as well. Thus, we find that the increase of the angular offset α_{off} as a function of p_r , that is ob-

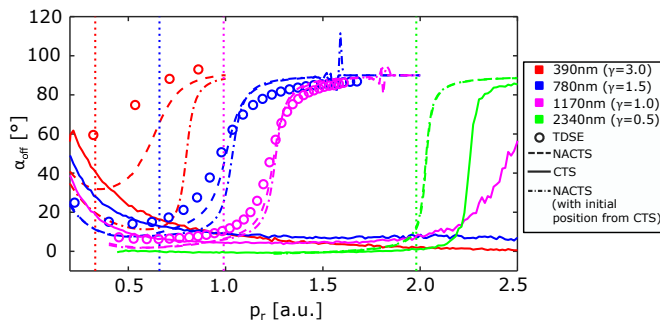


FIG. S2. The angular offset α_{off} is extracted from TDSE simulations (open circles), the NACTS model (dashed lines), the CTS model (solid lines) and the NACTS model using the initial position from the CTS model (dashed-dotted lines). Within the CTS model, the tunnel exit position from TIPIS is used (see Eq. (1)) as the initial position. The values for α_{off} are plotted as a function of the radial momentum p_r for different wavelengths as indicated in the legend. The corresponding Keldysh-parameters γ are also stated. Vertical dotted lines show the absolute value of the vector potential that corresponds to ionization at the peak of the electric field. The TDSE simulations are done as for Fig. 3 but without taking volume averaging into account. We have not done a TDSE simulation for the Keldysh-parameter $\gamma = 0.5$, but we expect the result to be consistent with the NACTS model. For all TDSE simulations in Fig. S2, an intensity of $9 \cdot 10^{13} \text{W/cm}^2$ is used. CEP averaging is done as in the main manuscript.

served in the main text, is universally present for a large range of laser parameters. To explore the relevance of non-adiabaticity, the NACTS model can be modified by using the initial positions from the TIPIS model instead of using the initial positions from SFA. The results are shown in S1(b) for $\gamma = 3$ and in Fig. S2 for four different values of γ . It is evident from Fig. S2 that the NACTS model that uses the initial positions from the TIPIS is

in good agreement with the NACTS model for $\gamma < 1$. In this parameter region, the momentum change that is due to the acceleration in the laser field (proportional to the vector potential) is large compared to the change in momentum that is due to the influence of the Coulomb interaction, that the electron experiences on its classical trajectory. Hence, the momentum distributions are only weakly influenced by Coulomb interaction. This observation agrees with the findings of the Rutherford-Keldysh-Model [4] and the analytical R-Matrix theory [5]. However, for smaller wavelengths (resulting in a smaller magnitude of the vector potential and higher values of γ) the momentum change that is due to Coulomb interaction is relevant. In this case, the initial positions strongly affect the offset angle α_{off} . In conclusion, the NACTS model leads to a significant improvement in modelling the correct dependence of the angular offset α_{off} as a function of the radial momentum p_r as compared to the CTS model.

* simon.brennecke@itp.uni-hannover.de

† eckart@atom.uni-frankfurt.de

- [1] S. Popruzhenko and D. Bauer, Strong field approximation for systems with Coulomb interaction, *J. Mod. Opt.* **55**, 2573 (2008).
- [2] S. V. Popruzhenko, G. G. Paulus, and D. Bauer, Coulomb-corrected quantum trajectories in strong-field ionization, *Phys. Rev. A* **77**, 053409 (2008).
- [3] H. Ni, N. Eicke, C. Ruiz, J. Cai, F. Oppermann, N. I. Shvetsov-Shilovski, and L.-W. Pi, Tunneling criteria and a nonadiabatic term for strong-field ionization, *Phys. Rev. A* **98**, 013411 (2018).
- [4] A. W. Bray, S. Eckart, and A. S. Kheifets, Keldysh-Rutherford model for the attoclock, *Phys. Rev. Lett.* **121**, 123201 (2018).
- [5] J. Kaushal and O. Smirnova, Nonadiabatic coulomb effects in strong-field ionization in circularly polarized laser fields, *Phys. Rev. A* **88**, 013421 (2013).